Astron. Astrophys. 357, L37–L40 (2000)

ASTRONOMY AND ASTROPHYSICS

LETTER

Letter to the Editor

Magnetic field structure of the cometary HII region G34.3+0.2

Magnetic field structure of G34.3+0.2

X. Zheng[1,2]**, M.J. Reid**[2]**, and J.M.Moran**[2]

[1] Nanjing University, Department of Astronomy, Nanjing 210093, P.R. China
[2] Harvard-Smithsonian Center for Astrophysics, 60 Garden Street, Cambridge, Massachusetts 02138, USA

Received 23 September 1999 / Accepted 20 April 2000

Abstract. We observed the hydroxyl (OH) masers in the ground-state 1665 and 1667 MHz transitions toward the cometary HII region G34.3+0.2 with the Very Long Baseline Array (VLBA). Our observations were sensitive to both right and left circular polarizations with a spectral resolution of 0.176 km s^{-1} and an angular resolution of 8×31 mas. We detected 120 maser features in a region of 3×6 arcsec, including 15 Zeeman pairs separated by an average distance of only 2 mas were identified. The OH masers are associated with two newly formed stars in the G34.3+0.2 complex. One star ionizes a weak, ultra-compact HII region (source B) and has a magnetic field orientation predominantly away from us. The other star, or stars, power the dominant cometary HII region (source C) and the magnetic field along the northern rim of the cometary source is directed toward us.

Key words: masers – polarization – stars: formation – ISM: individual objects: G34.3+0.2

1. Introduction

The archetypical "cometary" HII region G34.3+0.2, first characterized by Reid & Ho (1985), presents a prominent system with a bright "coma" and a parabolic-shaped ionisation front with an extremely sharp "upstream" edge and a weaker tail extending for about $40''$. The cometary morphology of some UC H II regions can be explained in a variety of ways. Initially, Reid and Ho suggested that the cometary morphology could be caused by the relative motion of the exciting star and the surrounding molecular material. In particular, they noted that a large expanding shell of gas associated with the stellar precursor to the W44 supernova might supply a significant component of the relative motion. Detailed bow-shock models have been elaborated by Van Buren et al. (1990) and Mac Low et al. (1991). These authors postulate that for a cometary UC H II region the ionised and molecular gas approach each other with a speed of order 10 km s^{-1} and their interaction forms a molecular bow shock supported by the wind from the ionising star(s). Alternatively, other authors suggested a "champagne flow" model (Tenorio-Tagle 1979; Bodenheimer, Tenorio-Tagle, & Yorke 1979; Tenorio-Tagle, Yorke & Bodenheimer 1979; Bedijn & Tenorio-Tagle 1981; and Yorke, Tenorio-Tagle & Bodenheimer 1983). In this model, an UC H II region is embedded in a molecular cloud with a large pressure gradient, and the ionised material expands rapidly in the direction of lower pressure. Finally, Gaume et al. (1994) suggest that the structure of the cometary HII region in G34.3+0.2 may be affected by ionised outflows from two other stars, G34.3+0.2A and B, embedded in the complex.

In a previous paper (Zheng, Moran & Reid 2000, hereafter Paper I), we discussed the distribution in space and velocity of masers in an "arc" paralleling the head of the cometary HII region based on earlier VLBI observations. Since magnetic fields play an extremely important role in star forming regions and may affect the dynamical properties of the region G34.3+0.2, we re-observed this source with the Very Long Baseline Array (VLBA) to map the polarized OH emission with sufficient angular resolution of (~ 10 mas) to resolve most maser clusters. These observations yielded a total of 120 maser features, from which we found 15 Zeeman pairs with the position differences between oppositely polarized masing features of less than 2 mas. This letter presents the magnetic field structure of two HII regions in the G34.3+0.2 complex.

2. Observations and results

The observations were conducted on 3 June 1995 with the VLBA operated by NRAO. [1] We observed the OH emission in both the 1665 and 1667 MHz transitions, in both right and left circular polarization. A 250 kHz passband centered on $V_{\rm LSR} = 60$ km s^{-1} was divided into 256 spectral channels, providing a Doppler velocity spacing of 0.176 km s^{-1}.

The calibration procedures are similar to those discussed in Paper 1, except for some extra steps needed to register the maps in both transitions and polarizations. Prior to normal calibration steps, we corrected the data for feed orientation changes (i.e.,

[1] The National Radio Astronomy Observatory is a facility of the National Science Foundation operated under cooperative agreement with Associated Universities, Inc.

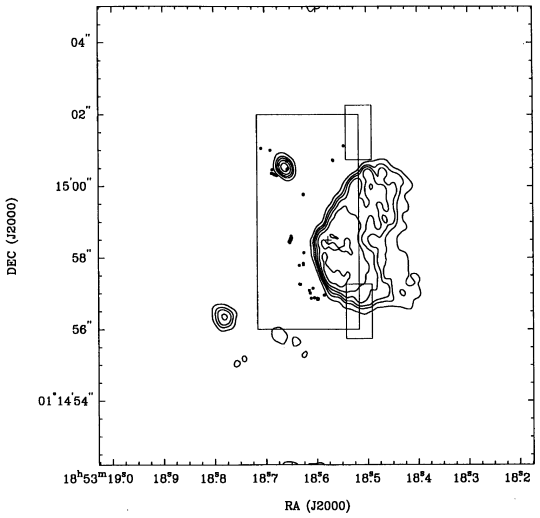

Fig. 1. A map of the distribution of OH maser features superimposed on the 23 GHz continuum (Argon et al. 1999). The absolute alignment between masers and continuum is taken from the VLA study of Argon et al. The continuum contour levels are 6, 12, 17, 24, 34 and 48 mJy. Solid dots show the maser features in the 1665 and 1667 MHz transitions in both right and left circular polarization. The rectangles delineate regions which we mapped and found OH emission.

parallactic angle rotation). A strong and simple point source at an LSR velocity of 58.8 km s^{-1} in the 1667 MHz RCP spectrum was selected as a phase reference feature. Fringe-fitting was performed on this feature to determine the residual fringe phase as a function of time. This was applied to all spectral channels in both polarizations in transitions. The calibrated visibilities were Fourier transformed and deconvolved using the AIPS task IMAGR. A 3×6 arcsec (E $\times$ N) field was mapped with a pixel size of 3×6 mas and the synthesized beam was 8×31 mas at a position angle -37° East of North. Individual channel maps had a noise level of about 10 mJy per beam. We identified maser features when they were detected over at least three adjacent spectral channels. For these features the position offsets relative to the reference feature, the FWHM and the peak intensity were fitted with a two-dimensional Gaussian brightness distribution.

Fig. 1 shows the spatial distribution of the identified OH maser features projected onto a contour plot of 1.3 cm continuum (Argon at al. 1999). Fig. 2a and 2b show the locations of the 1665 and 1667 MHz maser features, respectively. The appearance of the 1665 MHz maser features is similar to that observed by Gaume and Mutel (1987). These OH masers can be grouped as associated with two different newly formed stars: one group is clustered near the HII region source B in the north-east corner of the map near offset-coordinates (400,2000) mas. The source B cluster contains the strongest 1665 MHz masers in the entire region. This cluster is probably related to a young ionizing star that is physically distinct from the more energetic star that ionizes the cometary HII region. All other OH masers, including the 1667 MHz masers shown in Fig. 2b, are aligned along an arc that parallels the head of the cometary HII region. Maser spots in the northern section of the arc are less numerous but possibly better aligned with the limb-brightened parabolic

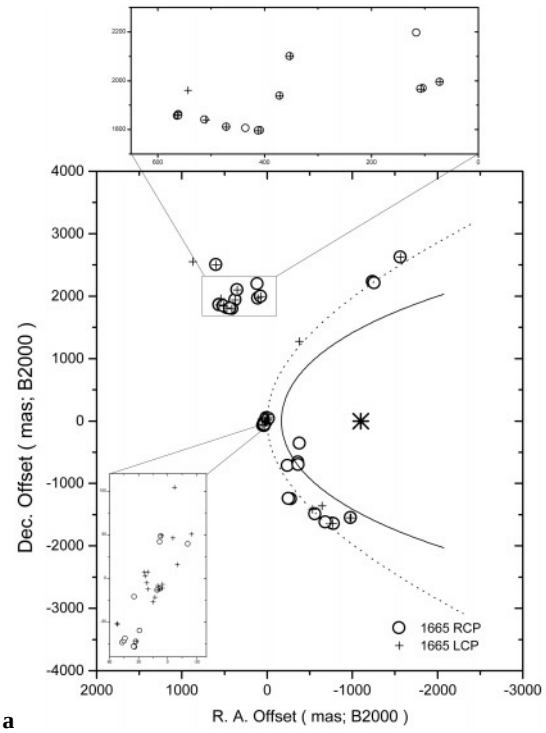

a

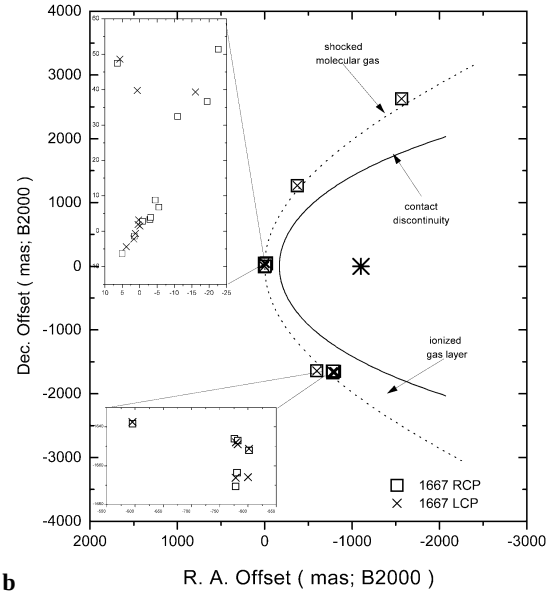

b

Fig. 2a and b. Maps of the relative positions of the OH maser features. (**a**) The RCP and LCP components of the 1665 MHz transition. (**b**) The RCP and LCP components of the 1667 MHz transition. The solid and dashed lines delineate the ionisation front and the contact discontinuity expected by the bow shock model. The asterisk indicates the position of the continuum peak.

shell than those in the southern part of the arc, which display a greater spread perpendicular to the arc. Masers in both sections may lie in a thin shell and the spread could result from projection effects.

The RCP and LCP components from a single physical condensation or cloudlet are usually referred to as a Zeeman pair (e.g., Moran et al. 1978, Reid et al. 1980, Carcia-Barreto et

Table 1. Zeeman pairs in G34.3+0.2

V(LSR) (km $^{-1}$)	Δ_α (mas)	σ (mas)	Δ_δ^{a} (mas)	σ (mas)	V(LSR)^{b} (km $^{-1}$)	Δ_α (mas)	σ (mas)	Δ_δ (mas)	σ (mas)	D^{c} (mas)	B^{d} (mG)
1665 RCP					1665 LCP						
62.6	103.74	0.03	1968.48	0.06	60.0	107.34	0.03	1965.90	0.00	4.43	4.4
60.9	560.97	0.30	1861.98	0.78	55.8	509.61	0.09	1840.44	0.24	2.04	8.6
60.7	371.37	0.03	1938.18	0.06	59.3	561.24	0.12	1859.94	0.24	0.36	2.4
60.5	-1565.64	0.06	2622.72	0.12	62.8	-1566.69	0.03	2623.32	0.06	1.21	-3.9
59.6	411.45	0.03	1795.56	0.06	56.5	412.38	0.15	1795.62	0.30	0.93	5.3
59.3	471.09	0.09	1810.74	0.24	55.9	471.09	0.06	1810.98	0.12	0.24	5.8
59.1	71.94	0.03	1994.52	0.06	58.9	71.82	0.00	1995.24	0.00	0.73	0.3
58.9	511.92	0.12	1840.50	0.30	55.8	509.61	0.09	1840.44	0.24	2.31	5.3
57.4	-769.41	0.24	-1643.04	0.72	57.7	-769.83	0.24	-1640.82	0.36	2.26	-0.5
55.8	-982.32	0.09	-1549.02	0.18	55.6	-974.61	0.03	-1549.26	0.12	7.71	0.3
59.8	598.23	0.03	2500.26	0.06	64.4	599.13	0.09	2499.30	0.24	1.32	-7.8
1667 RCP					1667 LCP						
60.9	-1565.55	0.03	2623.20	0.06	62.3	-1565.85	0.03	2623.44	0.06	0.38	-4.0
60.5	5.01	0.12	-6.30	0.42	60.7	3.87	0.03	-4.38	0.12	2.23	-0.5
58.2	-19.41	0.09	36.72	0.18	58.2	-16.02	0.18	39.36	0.42	4.30	0.5
52.1	-372.03	0.06	1264.50	0.12	53.5	-374.40	0.09	1268.34	0.18	4.51	-4.0

Footnotes: [a] Position offsets in right ascension and declination were determined by the Gaussian fitting in the amplitude peak channels. [b] The velocity of the amplitude peak of the features. [c] Angular distance between two features in a Zeeman pair. [d] Inferred magnetic field strength. The conversion from the velocity separation of the RCP and LCP components to magnetic field assumed 0.590 and 0.354 km s^{-1} mG^{-1} for the 1665 and 1667 transitions, respectively. Positive (negative) magnetic field values indicate that field points away (toward) from the observer.

al. 1988, Baudry & Diamond 1996). However, one rarely finds Zeeman pairs where the RCP and LCP components coincide to a small fraction of the spot size. We examined all possible pairings of oppositely circularly polarized features and identified 15 Zeeman pairs which are listed in Table 1. The polarized masing components identified as Zeeman pairs comprise 25% of all masing features detected. Most of the 90 masing features which could not be identified as part of a Zeeman pair are located in the region close to the vertex of the cometary HII region. Possibly a combination of magnetic field and velocity gradients results in greater amplification of one component of a Zeeman pair compared to the other, resulting in the detection of only one component.

The values in column 11 of Table 1 indicate the angular separations between the RCP and LCP components. These are among the best matched Zeeman pairs for any interstellar OH masers. The measurement uncertainty was typically less than 1 mas for the angular separations We required that the spatial separation of a Zeeman pair be less than 3×10^{15} cm clustering scale found for W3OH by Reid et al. (1980). For G34.3+0.2 at a distance of 3.8 kpc this corresponds to about 50 mas. However, the separations between RCP and LCP components average only 2 mas, or 10^{14}cm. The uncertainty in the velocity difference was typically less than about 0.2 km s^{-1} resulting in a magnetic field error of less than about 0.5 mG.

The magnitude of the magnetic fields, calculated from the velocity separation of the Zeeman pairs, ranges from -7.8 mG to $+8.6$ mG. The sign of the value indicates the line-of-sight direction of magnetic field, with positive sign corresponding to the RCP component having a higher velocity than the LCP component and the field pointing away from the observer. The vast majority of the Zeeman pairs associated with HII region B have positive magnetic field values. However, the pairs associated with the cometary HII region tend to have negative magnetic field values, further supporting the physical independence of these two sources.

3. Discussion

3.1. Spatial distribution

The high spatial resolution and dynamic range of our image allow us to obtain several new results: First, all OH maser spots seem to be well aligned along the parabolic ionisation front and the distribution of OH maser spots delineates the shape of the shocked gas. Second, we find that there is a strong OH maser cluster near the apex of the arc. The angular distance between the cluster and the continuum peak is $\approx 1\overset{''}{.}1$, corresponding to a projected distance of $\approx 6.3 \times 10^{16}$ cm. The cluster lies on the symmetry axis, which passes through the peak or "head" of the cometary HII component (component C). There are 55 OH maser spots in the cluster including the strongest maser components in the right circularly polarized emission of the 1665 MHz transition and both right and left circular polarized emission of the 1667 MHz transition. The expanded view of the cluster near the apex (see the inserted boxes in Fig. 2) show possible filamentary or "sheet-like" structures in the shocked gas. In the 1667 MHz transition one of these structures appears as a long, thin series of maser features, but we did not detect a systematic velocity gradient as would be expected were this an edge-on, rotating, disk-like object. The thickness of the shocked molecular gas is ≈ 22 mas, or $\approx 1.2 \times 10^{15}$ cm for a source distance 3.8 kpc. Third, the OH maser spots along the arc tend to cluster in clumps rather than uniformly distributed; this is particularly distinct in the northern part of the arc. The separations of adjacent clusters are greater than 600 mas and less than 1500 mas.

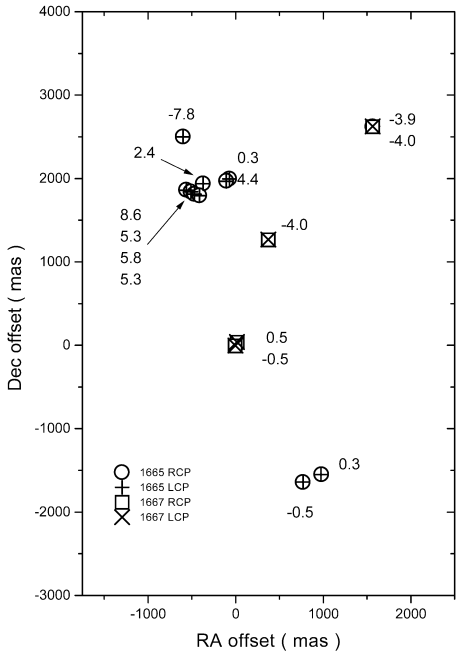

Fig. 3. Structure of the magnetic field in the G34.3+0.2 region. The numbers near the Zeeman pairs show the magnetic field strength. The conversion from the velocity separation of the RCP and LCP components to the field strength assumed 0.590 and 0.354 km s^{-1} mG^{-1} for the 1665 and 1667 MHz transitions, respectively. Positive (negative) magnetic field values indicate that field points away (toward) from the observer.

Speculations as to the origins of this clumping include fluid instabilities in the shocked gas shell (e.g., Gwinn 1994, Garcia-Segura & Franco 1996) and the separations between the clusters might be related to a scale of corrugations of C-shocks (Wardle 1990).

3.2. Magnetic field structure

Fig. 3 is a plot of the magnetic field strengths and orientations in the G34.3+0.2 HII region complex. Eight Zeeman pairs associated with HII region B exhibit an average field 4.2 mG. While seven of the eight pairs indicate a magnetic field pointed away from us, there is considerable variation in the strength of the magnetic field and, indeed, one Zeeman pair indicating a field oriented towards us. However, overall this region does contain a partially ordered magnetic field structure.

Turning now to the cometary HII region masers, we note that the northern part of the arc has magnetic fields of -4 mG. However, at the vertex and in the southern part of the cometary HII region, magnetic fields are generally small ($|B| < 1$ mG) when measured. The bow shock model in its simplest form would suggest an axially symmetric field configuration. This is not indicated by the data. The velocity distributions in the southern and northern maser clumps are not uniform, nor are the velocities seen in recombination lines for the ionized component (see Paper I for a more complete discussion). This complex distribution of magnetic field strength and velocities suggests a significantly anisotropic medium.

3.3. Polarization in OH masers

Very high circular polarization in OH maser emission has been recognized in many star-forming regions (Davies et al. 1966; Moran et al. 1978; Reid et al. 1980: Garcia-Barreto et al. 1988). Polarization in OH masers is caused by the presence of a directed magnetic field. The Zeeman effect splits the OH spectral lines, producing pairs of right and left circularly polarized (σ-component) lines. In a small number of sources one also detects linearly polarized π-components.

For the best studied source W3(OH), Garcia-Barreto et al. (1988) found 65 VLBI maser spots ($\approx 80\%$ of the total number) which were nearly 100% circularly polarized. However, only five pairs of oppositely circular polarized spots were detected within a small fraction of the spot sizes. The small number of Zeeman pairs detected could be due to gradients in velocity and magnetic field strength over the amplification length, which shift the line frequency by an amount comparable to the maser line width (see Cook 1966; Moran et al. 1978). Alternatively, maser amplification is non-linear, and small changes in the magnetic sub-level populations can lead to significantly different amplification for one component of a Zeeman pair compared to the other component.

Acknowledgements. The work at the CfA was made possible by support from the visiting scientist program of the Smithsonian Institution. XZ would like to thank L.J. Greenhill and A.S. Trotter for their help in the VLBA data processing. We thank P.T.P. Ho for suggestions to the manuscript. We appreciate the referee, M.-M. Mac Low, for his helpful comments.

References

Argon, A. L., Reid, M. J., & Menten, K. M. 1999, In preparation
Baudry, A.,& Diamond, P. J., 1998, A&A, 331, 697
Cook A. H., 1966, Nature 211, 503
Cook A. H., 1968, MNRAS 140, 299
Davies R. D., de Jager G., Verschuur G. C., 1966, Nature 209, 974
Garay, G., Rodriguez, L. F., 1990, ApJ, 362, 191
Garcia-Segura, G., Franco, J., 1996, ApJ, 469, 171
Gaume, R. A., Fey, A. L., Claussen, M. J., 1994, ApJ, 430, 648
Gaume, R. A. & Mutel, R. L., 1987, ApJS, 65 193
Garcia-Barreto J.A., Burke B.F., Reid M.J., et al., 1988, ApJ, 326,954
Gwinn, C.R., 1994, ApJ, 429,241
Mac Low, M. -M., Van Buren, D., Wood, D. O. S., Churchwell, E., 1991, ApJ, 369, 395
Moran J.M., Reid M.J., Lada C.J., et al., 1978, ApJ 224, L67
Reid, M. J., Haschick, A. D., Burke, B. F., Moran, J. M., Johnston, K. J. & Swenson, G. W. Jr., 1980, ApJ, 239, 89
Reid, M. J., Ho, P. T. P., 1985, ApJ, 288, L17
Tenorio-Tagle, G., Yorke, H. W., Bodenheimer, P., 1979, A&A, 80, 110
Van Buren, D., Mac Low, M.-M., Wood, D. O. S., Churchwell, E., 1990, ApJ, 353, 570
Wardle, M., 1990, MNRAS, 246, 98
Yorke, H. W., Tenorio-Tagle, G., Bodenheimer, P., 1983, A&A, 127, 313
Yorke, H. W., Tenorio-Tagle, G., Bodenheimer, P., 1984, A&A, 138, 325
Zheng, X., Moran, J.M. & Reid, M. J., 2000, to appear in MNRAS.